厚生科学研究費補助金（萌芽的先端医療技術推進研究事業）
分担研究報告書

臨床試験導入用動物実験モデルの作製、siRNAのデザインならびに前臨床試験

分担研究者　（株）ジーンケア研究所　二見　和伸、古市　泰宏

研究要旨　これまでに我々は、ゲノム維持機構に関与するRecQL1ヘリカーゼ遺伝子に対するsiRNAを癌治療薬候補として開発を進めてきた。その結果、感受性の異なる癌細胞種が存在することを見出したため、新たに反応性の異なる標的遺伝子の探索を行った。癌組織特異的に発現が高い遺伝子群を選抜し、癌治療薬としての可能性を探るべく、siRNAをデザインし、種々の培養細胞に導入し効果濃度を算出した。また、マイクロアレイを用いて発現プロファイルを確認した。この結果、バックアップとして有望である新標的遺伝子KNTC2を見出した。

A.　研究目的

我々はゲノム維持機構に関与するRecL1Qヘリカーゼの癌治療薬としての可能性を探ってきたが、反応性の異なる癌細胞種の存在に鑑み、あわせてバックアップとして新たな標的遺伝子の探索を行った。本研究では、新規標的遺伝子に対するsiRNAを用いて抗癌活性評価を行い、RNA干渉を応用した新規核酸医薬の開発を目的とする。

B.　研究方法

最初に、正常組織および癌組織間で遺伝子発現の定量的な比較を行い、癌組織特異的に発現が亢進している遺伝子群を選抜した。

これらを癌治療のための標的候補遺伝子群とし、それぞれの標的遺伝子に対するsiRNAをデザインし、RNA干渉に伴う細胞増殖抑制効果について調べた。

さらに癌特異的に細胞死をもたらす機序を解析するため、タイムラプス顕微鏡によるデータ取得を行った。このムービー記録により、siRNA導入後に、癌細胞が死に至る様子の連続的観察が可能となった。また、推定される細胞死の機序は、免疫染色法およびフローサイトメーターによって確認した。

以上の細胞学的解析に加え、マイクロアレイによって各遺伝子の発現プロファイルを確認し、siRNA導入によって誘導される細胞死が標的遺伝子の発現抑制に伴うものであることを確かめた。また、オフターゲットのような副次的な反応に拠らないことも同時に確認した。

（倫理面への配慮）
ヒト遺伝子DNAや動物を用いた研究ではないので、倫理面については問題ない。

C. 研究結果

正常組織および癌組織由来のRNA抽出物間で、定量的なPCRによる遺伝子発現比較を行い、癌組織で特異的に発現が亢進している遺伝子を選抜した。これらの遺伝子は、主として細胞周期関連遺伝子であり、周期進行に伴い特異的に発現が亢進するものであった。

選抜した遺伝子のうち、候補遺伝子としてふさわしいと思われる数種を選抜し、siRNAをデザイン・合成した。これらを培養癌細胞株に導入し、癌細胞選択的に細胞死を誘導する遺伝子としてキネトコアの構成成分をコードしているKNTC2遺伝子を見出した。KNTC2遺伝子の発現は、分裂細胞に特異的であり、正常組織では、ほとんど発現を確認できなかった。

本遺伝子に対するsiRNAの効果を種々の細胞中で評価したところ、0.1-2nM程度の低濃度で細胞増殖を抑え、細胞死を誘導することを確認した。また、作用機序としては、タイムラプスおよびFACS解析により、M期での捕捉による細胞周期停止であることを見出した。

免疫染色法により癌細胞について解析してみると、KNTC2の発現を抑制することで、キネトコアの形成が行われなくなり、M期を進行させることができず、やがて細胞死（分裂死、Mitotic catastrophe）にいたることが判明した。一方、正常細胞では、細胞周期は停止し、M期への進入は癌細胞と同様に認められなかったが、それらの細胞が死ぬということはなかった。

マイクロアレイを使った解析からは、KNTC2の特異的発現抑制を確認し、他の副次的反応ではないことを確かめた。

D. 考察

細胞分裂に於いて、細胞周期のチェックポイントは厳密であり、DNAの損傷・その他の不具がある場合、スピンドルチェックによって、そのような細胞を捕捉し、排除する仕組みがある。今回、我々が見出したKNTC2は、紡錘糸結合の場であるキネトコア成分をコードし、発現を抑制することで、M期進行が阻止される（＝スピンドルチェック）。この状態に陥った細胞はやがてはカタストロフィーと称される強力な細胞死によって排除される。一方、正常細胞では、動原体形成が行われていないことを感知し、M期への進入を自ら阻止しているものと思われる。ここに関与するProphase

checkpoint は、多くの癌細胞では機能せず、そのことが癌細胞-正常細胞の KNTC2 siRNA に対する感受性を分けるものと考える。

E. 結論

今回、我々が見出した KNTC2 は、細胞分裂の進行に必須なキネトコアの構成成分コードし、これを RNA 干渉の標的とすることで癌細胞の増殖を効果的に阻止することを見出した。以上のことから、KNTC2 はバックアップ候補遺伝子として有望であると思われる。

F. 健康危険情報

G. 研究発表

1. 論文発表

○○○○○○○○○○○○○○○

2. 学会発表

村田絵里子、多田周右、二見和伸、古市泰宏、関政幸、榎本武美「RecQL1 siRNA の処理によるがん細胞死」日本薬学会東北支部会、第４５回大会(2006)

H. 知的財産権の出願・登録状況

1. 特許取得

○○○○○○○○○○○○○○○

2. 実用新案登録

○○○○○○○○○○○○○○○

3. その他（出願特許）

【発明の名称】抗癌剤増感剤

【出願日】平成１８年９月

【発明者】二見和伸、高木基樹、杉本正信

【出願人】株式会社ジーンケア研究所

【発明の概要】既存抗癌剤の作用を増感させる目的に用いる siRNA 標的遺伝子の用途特許。

特願 2006-265988

厚生科学研究費補助金（萌芽的先端医療技術推進研究事業）
分担研究報告書

標的バブルリポソームに最適化された低侵襲治療装置の開発

分担研究者　福岡大学　医学部解剖学教室　立花克郎

研究要旨
標的バブルリポゾームに最適化された低侵襲治療装置の開発

A. 研究目的

超音波エネルギーによる，生体作用、薬剤透過性亢進作用、細胞内遺伝子導入、など、既に多くの論文で最近報告されてきた。本研究の目的は、超小型の超音波発振セラミック技術を応用した超音波照射による遺伝子導入の検討およびその安全な低侵襲治療システムの確立にある。

B. 研究方法

実験1　正常ヒト表皮メラニン細胞を培養液と１％PSAを用いてCO2インキュベータ内で培養し、２～３次培養細胞をtrypsinを用いて細胞を剥離、OptiCellTM の一側面に播種した。OptiCellは標準マイクロプレートサイズのフレーム内に2つの光学的にクリアなガス透過性生着面を持ち、その間の細胞培養エリアは滅菌の上、シールされている。内部及び内容物には自己シール性のアクセスポートにより無菌操作が可能で、細胞増殖、顕微鏡観察、選別、分離、細胞トランスフェクション(遺伝子導入)などに利用した。

実験２　ヒト臍帯静脈内皮細胞と正常ヒト皮膚繊維芽細胞の Co-Culture Model を用いて、超音波照射群、薬剤投与群、超音波照射・薬剤投与併用群、対照群を設定して、VEGF 誘導下の管腔形成に与える影響を調べた。超音波機器は Sonopore 4000 を用いた。薬剤は血管新生阻害剤であるフマジリン誘導体、FR118487 及び抗腫瘍剤である paclitaxel, 5-FU 誘導体(5'-DFUR)を使用した。管腔形成能の評価は PC にて画像処理を行い定量的に検討した。

C. 研究結果

１）培養した正常ヒト表皮メラニン細胞を 5.0～15.0×10^4/ml の濃度で 48 時間 CO2 インキュベータ内で培養し、OptiCell の面積比で90%以上増殖させた。正常ヒト表皮メラニン細胞を面積

比で 90%以上増殖させた OptiCell に pEGFP-N1 を 22μl、超音波造影剤（マイクロバブル）を 100μl 注入し、この装置を用いて様々な出力設定下で超音波を照射した。出力設定は、周波数 1.011 MHz 、出力電圧 (v)、出力周期 0.5 Hz、デューティー比 25%、パルスタイプ rectangular pulse type、スイープタイプ type 1 、スイープ幅 12 % 、スイープ間隔 100 ms で行った。24 時間後 pEGFP-N1 の gene transfection を蛍光顕微鏡で観察したところ、0.4W に比べ 0.6W の照射群で 3 倍の遺伝子導入率が得られた。一方照射時間と遺伝子導入率の関係では、10 秒と 20 秒で最高値を得たが、その後低下した。2）超音波は低出力(1MHz, 1.0W/cm2) の条件下では、短時間照射は管腔形成を維持または促進する可能性を示したが、照射時間の延長とともに管腔形成を抑制した。3）超音波照射・薬剤投与併用群は、薬剤投与群に比較して有意に管腔形成抑制効果を示し、その効果は照射部のみならず照射部外にまで及んだ。4）抗腫瘍剤である paclitaxel 及び 5-FU 誘導体 (5'-DFUR) は、低濃度下で管腔形成抑制効果を示すことが確認された。

D. 考察

遺伝子導入率は超音波照射の強度に比例するが、必ずしも照射時間と相関せず、最適条件が存在することが解った。本実験で使われた超音波条件では 10-20 秒が最高値を示した。また実験 2 では超音波の血管新生阻害に関する薬剤（血管新生阻害剤及び抗腫瘍剤）作用増強効果が示唆された。超音波の管腔形成に関する血管内皮細胞への直接的な影響に関しては更なる究明が必要である。

E. 結論

本実験結果より超音波の細胞への影響、遺伝子導入率、バブルの超音波条件設定を検討する上で必要な実験システムが開発されたと考えられる。様々な超音波条件よる遺伝子導入率の比較検討が行われたが、今後さらにこの実験方法で超音波プローブ最適条件の再検討と新しいマイクロバブルの研究開発が期待される。

F. 健康危険情報

G. 研究発表

1. 論文発表

1. Tachibana K, Tachibana S Emerging technologies using ultrasound for drag delivery Emerging Therapeutic Ultrasound 131-166 2006

2. 立花克郎 超音波による治療放射線医科学 - 生体と放射線・電磁波・超音波学会出版センター 2007
3. 立花克郎 超音波による遺伝子導入療法、Drug Delivery System (DDS) (3章) 脳神経超音波マニュアル 2007
4. Feril LB Jr, Tachibana K Ultrasound in Medicine: To Search and diseased Tissues. Philippine Physics journal 28:67-72
5. Tachibana K, Feril LBJr. Using ultrasound For Drug Delivery. Philippine Physics journal 28:125-135
6. Sonoda S, Tachibana K, Uchino E, Okubo A, Yamamoto M, Sakoda K, Hisatomi T, Sonoda KH, Negishi Y, Izumi Y, Takao S, Sakamoto T. Gene transfer to corneal epithelium and keratocytes mediated by ultrasound with microbubbles. Invest Ophthalmol Vis Sci. Invest Ophthalmol Vis Sci. 47(2):558-564 2006
7. Kagiya G, Tabuchi Y, Feril LB Jr, Ogawa O, Zhao Q-L, Kudo N, Hiraoka W, Tachibana K, Umemura S, and Kondo T. Confirmation of enhanced expression of heme oxygenase-1 gene induced by ultrasound and its mechanism: Analysis by cDNA microarray system, real-time quantitative PCR, and western blotting. J Med Ultrasonics 33:3-10 2006
8. Tabuchi Y, Ando H, Takasaki I, Feril LB Jr, Zhao Q-L, Ogawa R, Kudo N, Tachibana K and Kondo T Identification of genes responsive to low intensity pulsed ultrasound in a human leukemia cell line Molt-4 Cancer letters 246:149-156 2006
9. Feril LB Jr, Kondo T, Tabuchi, Ogawa R, Zhao Q-L, Nozaki T, Toru Y, Kudo N, and Tachibana K Biomolecular effects of low intensity ultrasoud: apoptosis, sonotransfection, and gene expression. Jpn. J. Applied Phys Japanese Journal of Applied Physics (in press) 2007
10. Feril LB Jr, Tachibana K, Yamaguchi K, Ogawa K, Dantsuji Y, Irie Y and Endo H Bioeffects of Ultrasound for Therapy Philippine Physics Journal 29: (in press) 2007
11. 立花克郎、江本 精微小気泡と超音波による血栓溶解療法とDDSの動向 細胞 38(4):15-18 2006
12. 立花克郎、入江 豊、小川皓一 超音波の治療への応用 J Med

Ultrasound 33(6):631-639

13. Feril LB Jr, Kondo T, Tachibana K, Ogawa R and Ogawa K Biological Effects of Ultrasound : Sonomechanical Mechanism, and Its Implications on Therapy and Biosafety Therapeutic Ultrasound: 5th International Symposium on Therapeutic Ultrasound Cancer Science (in press) 2007
14. Emoto M, Tachibana K, Iwasaki H and Kawarabayashi T Antitumor Effect of TNP-470, an Angiogenesis Inhibitor, Combined with Ultrasound Irradiation for Human Uterine Sarcoma Xenografts Evaluated by Contrast Color Doppler Ultrasound Cancer Science (in press) 2007

2. 学会発表

1. 超音波の治療応用-新しいがん治療への利用法 日本放射線音響学会第49回大会 2006.9.6-8 北海道
2. 特別講演：コントラストエコーの治療への応用 第31回ｺﾝﾄﾗｽﾄｴｺｰ研究会 2006.8.12 さいたま市大宮
3. 超音波治療の現状 日本超音波医学会第32回東北地方会学術集 2006.9.24 秋田市
4. 超音波の治療応用ー新しいがん治療への利用法（ワークショップ）放射線影響学会第49回大会 2006.9.6-8 札幌
5. マイクロバブルの将来展望について 第9回日本栓子検出と治療学会 2006.11.25 京都（招待講演）

（海外）

1. In Vivo-Simulated Sonotransfection and the Effect of Gammā Interferon Gene on Neurofibroma Proliferatio ISTU 2006.9.30 ロンドン

H. 知的財産権の出願・登録状況

1. 特許取得
   特になし
2. 実用新案登録
   特になし
3. その他
   特になし

Koshiyama K, Kodama T	Structural change in lipid bilayers and water penetration induced by shock waves: molecular dynamics simulations.	Biophys J	Sep 15;91(6)	2198-205	2006
Tachibana K,	Emerging technologies using ultrasound for drag delivery	Emerging Therapeutic Ultrasound		131-166	2006
Feril LB Jr, Tachibana K	Ultrasound in Medicine: To Search and diseased Tissues.	Philippine Physics journal	28	67-72	2006
Tachibana K, Feril LBJr.	Using ultrasound For Drug Delivery.	Philippine Physics journal	28	125-135	
Sonoda S, Tachibana K, et al.	Gene transfer to corneal epithelium and keratocytes mediated by ultrasound with microbubbles.	Invest Ophthalmol Vis Sci. Invest Ophthalmol Vis Sci.	47(2)	558-564	2006
Kagiya G, Tachibana K, et al.	Confirmation of enhanced expression of heme oxygenase-1 gene induced by ultrasound and its mechanism: Analysis by cDNA microarray system, real-time quantitative PCR, and western blotting.	J Med Ultrasonics	33	:3-10	2006
Tabuchi Y, Tachibana K et al.	Identification of genes responsive to low intensity pulsed ultrasound in a human leukemia cell line Molt-4	1. Cancer letters:	246	149-156	2006

別紙４

研究成果の刊行に関する一覧表

書籍

著者氏名	論文タイトル名	書籍全体の編集者名	書　籍　名	出版社名	出版地	出版年	ページ

雑誌

発表者氏名	論文タイトル名	発表誌名	巻号	ページ	出版年
T Negishi, F Koizumi, Y Matsumura, et al.	NK105, a paclitaxel-incorporating micellar nanoparticle, is a more potent radiosensitizing agent compared to free paclitaxel.	Brit J Cancer	95	601-606	2006
F Koizumi, Y Matsumura. et al.	Novel SN-38-incorporated polymeric micelles, NK012, eradicate vascular endothelial growth factor-secreting bulky tumors.	Cancer Res	66	10048-10056	2006
Ryo Suzuki, Kazuo Maruyama:	Gene delivery by combi - nation of novel liposomal bubbles with perfluoropropane and ultra -sound	J. Control. Release	117	130-136	2007
Ryo Suzuki, Kazuo Maruyama	Development of the liposomes entrapped ultrasound imaging gas ("Bubble liposomes") as novel gene delivery carriers, AIP conference Proc.	Therapeutic ultrasound		568-572	2006
Takahashi M, Kodama T.	Spinal gene transfer using ultrasound and microbubbles.	J Control Release.	117(2)	267-272	2007
Kodama T.	A non-invasive tissue-specific molecular delivery method of cancer gene therapy.	Minim Invasive Ther Allied Technol	15(4)	226-229	2006

British Journal of Cancer (2006) 95, 601–606

www.bjcancer.com

NK105, a paclitaxel-incorporating micellar nanoparticle, is a more potent radiosensitising agent compared to free paclitaxel

T Negishi[1], F Koizumi[1], H Uchino[2], J Kuroda[1], T Kawaguchi[3], S Naito[2] and Y Matsumura[*,1]

[1]Investigative Treatment Division, Research Center for Innovative Oncology, National Cancer Center Hospital East, 6-5-1 Kashiwanoha, Kashiwa, Chiba 277-8577, Japan; [2]Department of Urology, Graduate School of Medical Sciences, Kyushu University, 3-1-1 Maidashi, Higashi-ku, Fukuoka, Fukuoka 812-8582, Japan; [3]Department of Anatomy and Histology, Fukushima Medical University School of Medicine, 1-Hikariga-oka, Fukushima, Fukushima 960-1247, Japan

NK105 is a micellar nanoparticle formulation designed to enhance the delivery of paclitaxel (PTX) to solid tumours. It has been reported to exert antitumour activity *in vivo* and to have reduced neurotoxicity as compared to that of free PTX. The purpose of this study was to investigate the radiosensitising effect of NK105 in comparison with that of PTX. Lewis lung carcinoma (LLC)-bearing mice were administered a single intravenous (i.v.) injection of PTX or NK105; 24 h after the drug administration, a proportion of the mice received radiation to the tumour site or lung fields. Then, the antitumour activity and lung toxicity were evaluated. In one subset of mice, the tumours were excised and specimens were prepared for analysis of the cell cycle distribution by flow cytometry. Combined NK105 treatment with radiation yielded significant superior antitumour activity as compared to combined PTX treatment with radiation ($P = 0.0277$). On the other hand, a histopathological study of lung sections revealed no significant difference in histopathological changes between mice treated with PTX and radiation and those treated with NK105 and radiation. Flow-cytometric analysis showed that NK105-treated LLC tumour cells showed more severe arrest at the G2/M phase as compared to PTX-treated tumour cells. The superior radiosensitising activity of NK105 was thus considered to be attributable to the more severe cell cycle arrest at the G2/M phase induced by NK105 as compared to that induced by free PTX. The present study results suggest that further clinical trials are warranted to determine the efficacy and feasibility of combined NK105 therapy with radiation.
British Journal of Cancer (2006) **95,** 601–606. doi:10.1038/sj.bjc.6603311 www.bjcancer.com
Published online 8 August 2006

Keywords: paclitaxel; NK105; radiosensitiser; polymer micelle; drug delivery system

Paclitaxel (PTX) has been demonstrated to be one of the most effective anticancer agents available at present (Carney, 1996; Khayat *et al*, 2000). Besides its antitumour activity, its ability to induce radiosensitisation has been reported both *in vitro* (Tishler *et al*, 1992; Choy *et al*, 1993; Lokeshwar *et al*, 1995; Rodriguez *et al*, 1995) and *in vivo* (Milas *et al*, 1994, 1995; Cividalli *et al*, 1998) this effect has been attributed to its effect of stabilising microtubules and inducing cell cycle arrest at the G2/M phase, the most radiosensitive phase of the cell cycle (Terasima and Tolmach, 1963; Sinclair and Morton, 1966). As several clinical studies have demonstrated the efficacy of PTX-based chemotherapy combined with radiotherapy, the combined modality is considered to be a potentially important treatment option for lung and breast cancer (Choy *et al*, 1998a, b, 2000; Dowell *et al*, 1999; Formenti *et al*, 2003; Kao *et al*, 2005).

The adverse effects of radiation, namely, lung toxicities in patients with breast or lung cancer treated by thoracic radiation, are of great concern, and may be dose limiting or even have a negative impact on the quality of life of the patients, even though radiation is an efficient treatment option. Lung toxicities often result in lung fibrosis, necessitating change of the treatment method and causing much distress or even death of the patients (Penney and Rubin, 1977; Early Breast Cancer Trialists' Collaborative Group, 2000; Lind *et al*, 2002). Some clinical trials actually reported an increased incidence of pneumonitis following combined PTX therapy with radiation in patients with breast or lung cancer (Taghian *et al*, 2001; Hanna *et al*, 2002; Chen and Okunieff, 2004).

Although widely used, PTX itself has several adverse effects, such as peripheral sensory neuropathy (Rowinsky *et al*, 1993; Rowinsky and Donehower, 1995), and its poor solubility in water is also associated with such effects as anaphylaxis and other severe hypersensitivity reactions attributable to Cremophor EL and ethanol, which are essential for solubilising PTX (Weiss *et al*, 1990; Rowinsky and Donehower, 1995). In order to overcome these problems, we prepared a new formulation, NK105, which is a PTX-incorporating polymeric micellar nanoparticle (85 nm in size) (Hamaguchi *et al*, 2005). NK105 is formed by facilitating the self-association of amphiphilic block copolymers constructed using polyethylene glycol (PEG) as the hydrophilic segment and modified polyaspartate as the hydrophobic segment in an aqueous medium. Owing to the PEG constituting the outer shell of the micelles, NK105 is soluble in water. In addition, PEG also confers a stealth property to the formulation, that allows the micellar drug preparation to be less avidly taken up by the reticuloendothelial

*Correspondence: Dr Y Matsumura; E-mail: yhmatsum@east.ncc.go.jp
Revised 5 June 2006; accepted 11 July 2006; published online 8 August 2006

system (RES) and to be retained in the circulation for a longer period of time (Klibanov *et al*, 1990, 1991; Allen, 1994; Gabizon *et al*, 1996). The prolonged circulation time and the ability of NK105 to extravasate through the leaky tumour vasculature (i.e., the EPR (enhanced permeability and retention) effect) causes accumulation of PTX in tumour tissues (Matsumura and Maeda, 1986; Maeda and Matsumura, 1989). We previously demonstrated that NK105 is associated with reduced neurotoxicity and also exerts more potent antitumour activity on human cancer xenograft, as compared to free PTX. In addition, because of its solubility in water, it is expected that the incidence of anaphylaxis and hypersensitivity reactions attributable to Cremophor EL and ethanol may also be reduced with NK105. A clinical trial of NK105 is now under way.

In this context, it is expected that the use of NK105 in place of PTX in combination with radiation may also yield superior results, because of the more potent antitumour activity of this drug as compared to that of free PTX. In this study, we evaluated the antitumour activity and severity of lung fibrosis induced by PTX and NK105 administered in combination with thoracic radiation, to examine whether combined NK105 chemotherapy with radiation would be an acceptable or useful treatment modality.

MATERIALS AND METHODS

Mice

Eight-week-old female C57BL/6J mice were purchased from Charles River Japan Inc. (Kanagawa, Japan). All the animal procedures were performed in compliance with the guidelines for the care and use of experimental animals, drawn up by the Committee for Animal Experimentation of the National Cancer Center; these guidelines meet the ethical standards required by law and also comply with the guidelines for the use of experimental animals in Japan.

PTX and NK105

Paclitaxel was purchased from Merican Corp. (Tokyo, Japan). NK105 is a PTX-incorporating 'core-shell-type' polymeric micellar nanoparticle formulation that was prepared by a previously reported procedure (Hamaguchi *et al*, 2005). Briefly, polymeric micellar particles were formed by facilitating the self-association of amphiphilic block copolymers in an aqueous medium. The polymer of NK105 was constructed using PEG as the hydrophilic segment and modified polyaspartate as the hydrophobic segment. The carboxylic groups of the polyaspartate block were modified by the esterification reaction with 4-phenyl-1-butanol, resulting in conversion of half of the groups to 4-phenyl-1-butanolate. Molecular weight of the polymers was determined to be approximately 2000 (PEG block: 12 000; moditied polyaspartate block: 8000).

Via the self-association process, PTX was incorporated into the inner core of the micelle system by physical entrapment through hydrophobic interactions between the drug and specifically well-designed block copolymers for PTX. NK105 was obtained as a freeze-dried formulation and contained ca.23% (WW^{-1}) of PTX. Finally, NK105, PTX-incorporating polymeric micellar nanoparticle formulation with a single and narrow size distribution, was obtained. The weight-average diameter of the nanoparticles was approximately 85 nm ranging from 20 to 430 nm.

Irradiation

The mice were anesthetised by intraperitoneal (i.p.) injection of nembutal (75 mg kg^{-1}) and placed on the stage for irradiation. The whole thorax or subcutaneous (s.c.) tumours of the thigh were irradiated using a Faxitron cabinet X-ray system model CP-160 by 100 kV X-rays from a linear accelerator, at a dose rate of 2 Gy min^{-1}. Totally 12 Gy was irradiated to each mouse. The whole body except irradiated parts, lung field or tumour lesion, were shielded with specially designed lead blocks.

Flow cytometry

At 24 h after the injection of PTX or NK105 into the Lewis lung carcinoma (LLC) tumour-bearing C57BL/6j mice, the tumours were excised, minced in PBS, and fixed in 70% ethanol at 4°C for 48 h. After being fixed, the tumours were digested with 0.04% pepsin (Sigma chemical co., St Louis, MO, USA) in 0.1 N HCl for 60 min at 37°C in a shaking bath for preparing single-nuclei suspensions. The nuclei were then centrifuged, washed twice with PBS, and stained with 40 $\mu g\,ml^{-1}$ of propidium iodide (Molecular Probes, OR, USA) in the presence of 100 $\mu g\,ml^{-1}$ RNase in 1 ml PBS for 30 min at 37°C. The stained nuclei were analysed with a B-D FACSCalibur (BD Biosciences, San Jose, CA, USA). The cell cycle distribution was analysed using the Modfit program (Verity Software House Inc., Topsham, ME, USA).

Evaluation of the antitumour activity

For this experiment, 3×10^6 LLC cells were inoculated s.c. into the right thighs of mice. The tumour volume was calculated using the formula, tumour volume (mm^3) $= a \times b^2/2$ (a = longest tumour diameter, b = shortest tumour diameter). When the tumour volume reached approximately 100 mm^3 on day 14 after the tumour inoculation, the mice were randomly allocated to test groups of about four or five mice each, and started the treatment on the same day. There were six test groups, as follows: untreated control, PTX treatment alone, NK105 treatment alone, radiation alone, combined PTX treatment with radiation, and combined with NK105 treatment with radiation.

In the groups receiving PTX or NK105, the mice were administered a single intravenous (i.v). injection of PTX or NK105 at the dose of 45 mg kg^{-1}; 24 h after the drugs were administered, the tumour sites of the mice in the groups scheduled to receive radiation were irradiated.

The antitumour activity of each treatment regimen was evaluated by measuring the tumour volume. Tumour volume and body weight was measured every 3 days.

Evaluation of lung toxicity

The severity of lung toxicity was evaluated histologically in the following test groups; untreated control ($n=6$), radiation treatment alone ($n=6$), combined PTX treatment with radiation ($n=9$), and combined NK105 treatment with radiation ($n=10$). Mice were administered a single i.v. injection of PTX or NK105 at the dose of 45 mg kg^{-1}; 24 h after the drugs were administered, the thorax of the mice in the groups scheduled to receive radiation was irradiated. All the mice were killed 36 weeks after the drug administration. At the time of the killing, the lungs were removed, and the right lungs were fixed in 10% buffered formalin for 24 h, then embedded in paraffin. The lungs were inflated at 20 cm water pressure by intratracheal infusion of 10% buffered formalin before fixation. Sections (5 μm- thick) were stained with haematoxylin and eosin (H&E) and observed under the light microscope. The severity of the pulmonary fibrosis was assessed based on Ashcroft's scoring system (Ashcroft *et al*, 1988). Briefly, all the fields of each lung section were scanned under a Leica microscope at a magnification of ×100, then each field was visually graded from 0 (normal lung) to 8 (total fibrotic obliteration of the field). The mean grades obtained for all of the fields was then calculated as the visual fibrotic score.

Immunohistochemistry

The lung sections were deparaffinised and rehydrated, then microwaved in 0.01 M sodium citrate buffer for 15 min at 90°C to retrieve epitopes, and cooled at room temperature. An endogenous peroxidase blocking solution of 3% hydrogen peroxide was applied for 20 min at room temperature. After blocking the nonspecific binding sites with 2% normal goat serum, the sections were incubated with rabbit anti-mouse collagen III immunoglobulin G (IgG) (Chemicon International, Temecula, CA, USA) overnight at 4°C. The sections were then washed with PBS, followed by the addition of biotin-conjugated goat anti-rabbit IgG (Vector Laboratories Inc., Burlingame, CA, USA) and incubation for 30 min at room temperature. The sections were then washed and incubated with horseradish-peroxidase-conjugated avidin–biotin complex (Vector Laboratories Inc., Burlingame, CA, USA) at room temperature for 30 min, in accordance with the manufacturer's instructions (Vector Laboratories Inc.). The immunoreactions were visualised using 3,3′-diaminobenzidine as the substrate and counterstaining with haematoxylin.

Statistical analysis

Date were expressed the mean ± s.d. Differences between the test groups were analysed by Student's *t*-test. We used Stat View (SAS Institute Inc.) statistical software. A value of $P<0.05$ was considered statistically significant.

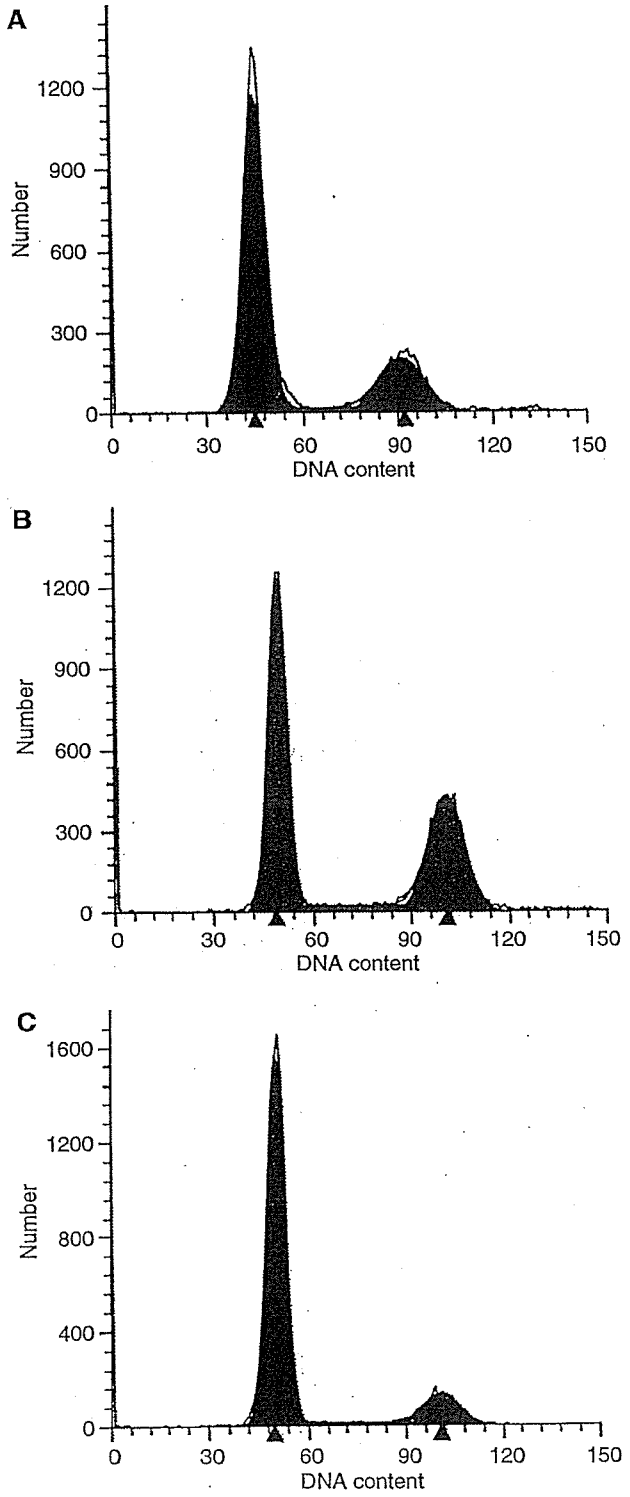

Figure 1 Cell cycle analysis. Cell cycle analysis of LLC tumour cells 24 h after PTX (**A**) or NK105 administration (**B**). Untreated control cells are shown in (**C**).

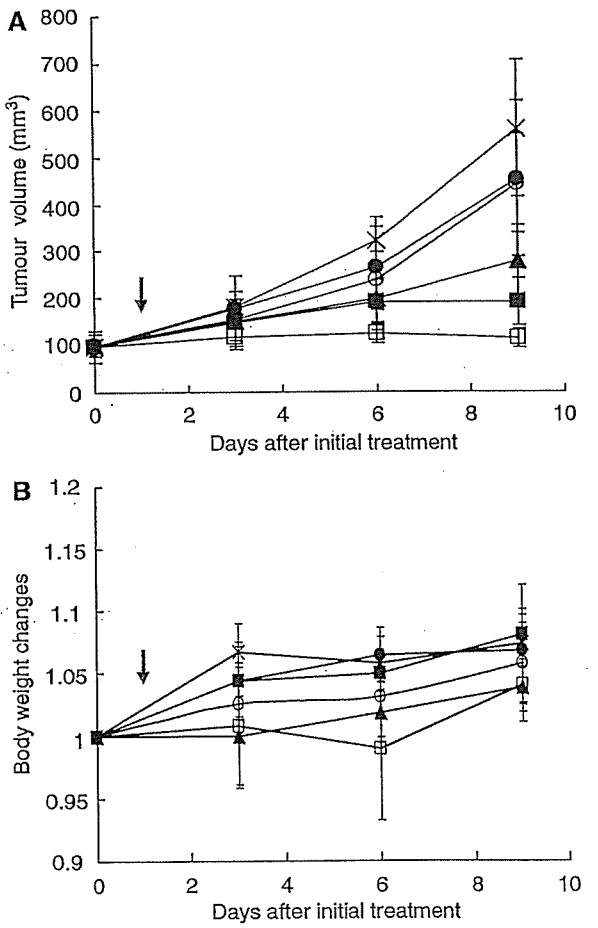

Figure 2 Antitumour activity. Changes in the LLC tumour growth rates in the mice. (**A**) Mice receiving TXL-alone (●), NK105-alone (○), combined treatment with PTX and radiation (■), and combined treatment with NK105 and radiation (□) were administered a single i.v. injection of PTX or NK105 at the dose 45 mg kg^{-1} on day 14 after the tumour inoculation (= on day 0 after the initial treatment). After 24 h the drugs were administered, the mice in the radiation-alone (△) and the combined-treatment groups were irradiated (arrow). Mice in the control group (×) were given no treatment. (**B**) Changes in the relative body weight. Data were derived from the same mice as those used in the present study.

RESULTS

Cell cycle analysis

At 24 h after the administration of PTX or NK105 to the LLC-tumour-bearing mice, severe cell cycle arrest at the G2/M phase was observed in the tumour cells treated with the drugs as compared with that in the control (no drug treatment) (Figure 1C). There was a tendency towards the NK105-treated LLC tumour cells (Figure 1B) showing more severe arrest at the G2/M phase than the PTX-treated cells (Figure 1A).

Antitumour activity

Decreased tumour growth rates of the LLC tumours were observed in the mice of the radiation alone, combined PTX with radiation, and combined NK105 with radiation groups. No antitumour activity was observed following treatment with either PTX or NK105 alone, because LLC is primarily a PTX-resistant tumour. Combined NK105 therapy with radiation yielded superior antitumour activity as compared to both radiation alone ($P=0.0047$) and combined PTX therapy with radiation ($P=0.0277$) on the day 9 after the treatment initiation (Figure 2A). No significant differences in body weight changes were noted among the groups tested (Figure 2B).

Lung toxicities

Histopathological examination of the lung sections of all the mice receiving radiation showed inflammatory cell infiltration, appearance of intra-alveolar macrophages, and destruction of the alveolar architecture. Major portions of the alveolar septa in the lung sections prepared from the irradiated mice showed slight thickening, although no massive structural destruction was observed (Figure 3A). On the other hand, the lung sections prepared from the control nonirradiated group showed no significant histopathological changes (Figure 3B). Ashcroft's fibrosis scores in the groups of mice that received radiation ranged from 0.975 to 1.426, with no significant differences among the groups. The score in the control group was nearly zero. In the groups receiving radiation, the severity of lung fibrosis differed significantly among the mice within the same groups, as did the Ashcroft's scores, that is, the s.d. of the Ashcroft's scores in the mice receiving radiation was very high (Figure 3C).

Type III collagen deposition

Immunohistochemical analysis of lung sections prepared from the mice receiving radiation revealed significant collagen deposition, especially in the subpleural regions, while that of lung sections prepared from the control group showed little collagen deposition. There were no significant differences among the different groups receiving radiation (Figure 3D).

DISCUSSION

It is well known that PTX enhances the radiosensitivity of tumour cells by inducing cell cycle arrest at the G2/M phase, the most radiosensitive phase of the cell cycle (Terasima and Tolmach, 1963;

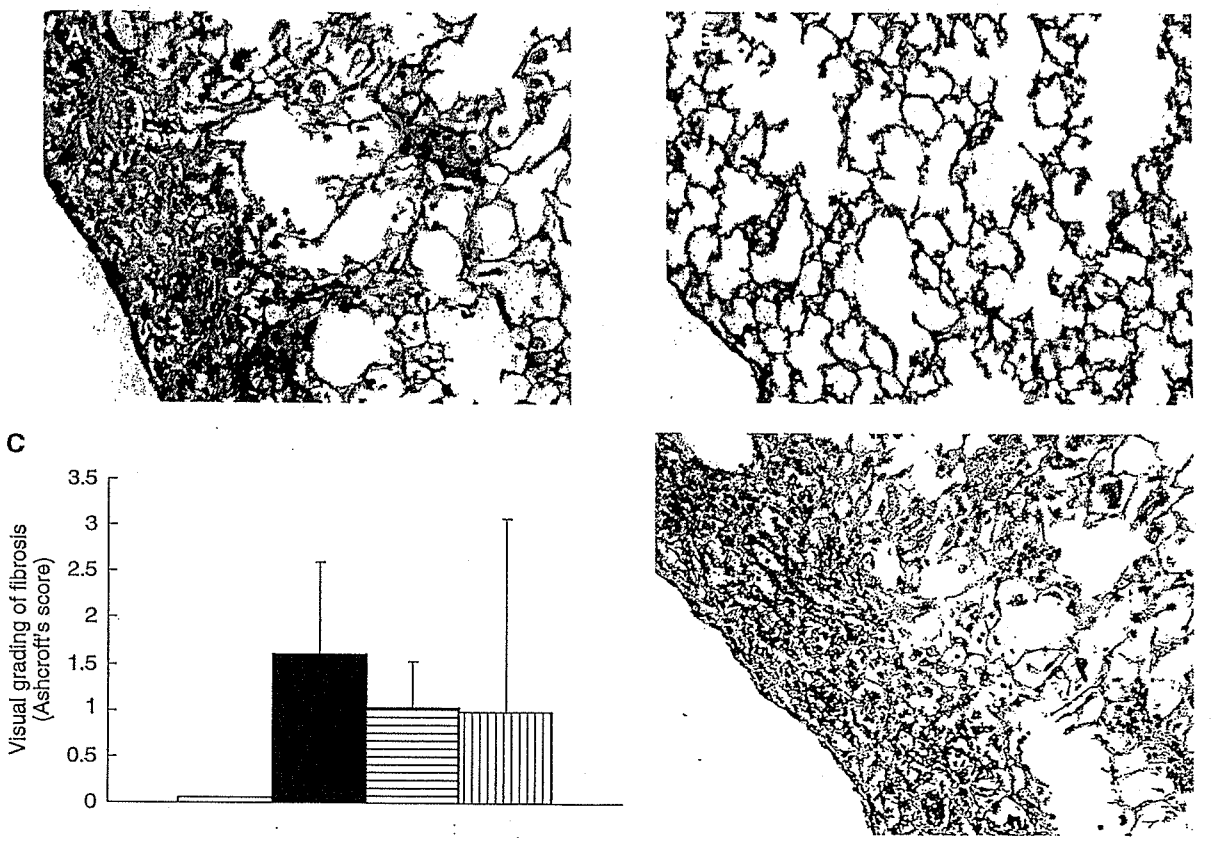

Figure 3 H&E staining of the lungs of C57BL/6J mice surviving 36 weeks after the thoracic radiation (**A**) and sham radiation (**B**). (**C**) Semiquantitative analyses to estimate the severity of pulmonary fibrosis in the mice receiving sham radiation (□), thoracic radiation alone (■), combined PTX with radiation (▤), and combined NK105 with radiation (▥). H&E- stained lung tissue sections were assessed to estimate the severity of pulmonary fibrosis by visual grading of fibrosis (Ashcroft's score). Collagen III staining of the irradiated lungs of mice (**D**).

Sinclair and Morton, 1966). Many reports have confirmed the radiosensitising effect of PTX in different cell lines (Tishler *et al*, 1992; Choy *et al*, 1993; Lokeshwar *et al*, 1995; Rodriguez *et al*, 1995), *in vivo* experiments (Milas *et al*, 1994, 1995; Cividalli *et al*, 1998), and in several clinical trials of combined PTX with radiation therapy according to different schedules (Dillman *et al*, 1990; Arriagada *et al*, 1991; Morton *et al*, 1991; Furuse *et al*, 1999; Sause *et al*, 2000; Chen *et al*, 2003). Chen *et al* (2003) examined the optimal timing of PTX treatment and irradiation in relation to the cell cycle, and recommended that radiation be given at least 5 h after PTX administration, because G2/M arrest of a lung cancer cell line was shown to start at 4 h after PTX treatment and to last for 44 h.

In our experimental model to evaluate the antitumour activity, the tumours were irradiated 24 h after a single i.v. injection of PTX or NK105. No significant increase in the antitumour activity as compared with that in the control (no treatment) was observed following a single i.v. injection of either PTX or NK105 at the dose of 45 mg kg^{-1}; LLC tumours are known to be primarily resistant to PTX. In fact, the IC_{50} of PTX against an LLC tumour cell line was shown to be 84.1 nM, which is about 10-fold higher than that of NK105 against various cancer cell lines tested in our previous work (Hamaguchi *et al*, 2005). Combined NK105 therapy with radiation yielded superior antitumour activity as compared with radiation alone or combined PTX therapy with radiation. This result suggests that NK105 has a more potent radiosensitising effect than PTX. In our study, there was a tendency towards NK105-treated LLC tumour cells showing more severe arrest at the G2/M phase as compared to PTX-treated cells at 24 h after the injection of the drugs, the timing of the radiation treatment, probably because NK105 allows a higher concentration of PTX to be maintained in the tumour than conventional PTX (Hamaguchi *et al*, 2005). We suppose that this is the reason why NK105 exerted more potent radiosensitising activity than PTX.

Next, we were concerned about the adverse effects of combined NK105 therapy with radiation. New micellar drugs are designed based on the idea that DDS can accumulate in the tumour selectively, while showing reduced distribution in normal tissues. We demonstrated that the incorporation of cisplatin into micelles significantly reduced the nephrotoxicity and neurotoxicity of cisplatin (Uchino *et al*, 2005). However, it was also shown that micelle- incorporated cisplatin caused transient liver dysfunction because it was trapped more avidly by the RES as compared to free cisplatin, even though the PEG of the outer shell of the micelle confers the so-called stealth effect.

In this study, our examination of the lung sections of mice treated with NK105 and radiation revealed that the histopathological changes such as inflammatory cell infiltration, appearance of intra-alveolar macrophages, and destruction of the alveolar architecture were induced by thoracic radiation and not by the accumulation of NK105 in the lung. There were no significant differences in the histopathological changes observed among the mice treated by NK105 and radiation and mice treated by radiation alone or PTX with radiation. The severity of lung fibrosis did not differ significantly among the test groups either. Although some clinical trials reported an increased incidence of pneumonitis and esophagitis following combined PTX therapy with radiation (Taghian *et al*, 2001; Hanna *et al*, 2002; Chen and Okunieff, 2004), others reported no influence on the incidence of such adverse effects (Ellerbroek *et al*, 2003; Yu *et al*, 2003). Several clinical trials and *in vivo* experiments have discussed the subject, however, no definitive conclusion has been arrived at (Mason *et al*, 1995; Choy *et al*, 1998; Yu *et al*, 2004; Kao *et al*, 2005). In our study, in regard to the incidence of esophagitis, there were no significant differences in the histopathological changes observed in the esophageal sections at one week after the treatment among the test groups (data not shown).

In conclusion, we demonstrated that combined NK105 chemotherapy with radiation exerts significant antitumour activity. Furthermore, the lung toxicity of this combined treatment modality was also acceptable as compared with that observed following radiation alone or combined PTX therapy with radiation. However, further studies are necessary to determine the effectiveness of NK105 in terms of its radiosensitising effect.

ACKNOWLEDGEMENTS

We thank Drs K Sugiyama and K Tsuchihara for their scientific advice and Mrs C Kanai and Mrs N Mie for their technical assistance. We are also grateful to Mrs K Shiina for her secretarial assistance. This work was supported by a Grant-in-Aid from the Ministry of Health, Labor and Welfare of Japan (Y Matsumura) and a Grant-in-Aid for Scientific Research on Priority Areas from the Ministry of Education, Culture, Sports, Science and Technology (Y Matsumura).

REFERENCES

Allen TM (1994) Long-circulating (sterically stabilized) liposomes for targeted drug delivery. *Trends Pharmacol Sci* 15: 215–220

Arriagada R, Le Chevalier T, Quoix E, Ruffie P, de Cremoux H, Douillard JY, Tarayre M, Pignon JP, Laplanche A (1991) ASTRO (American Society for Therapeutic Radiology and Oncology) plenary: Effect of chemotherapy on locally advanced non-small cell lung carcinoma: a randomized study of 353 patients. GETCB (Groupe d'Etude et Traitement des Cancers Bronchiques), FNCLCC (Federation Nationale des Centres de Lutte contre le Cancer) and the CEBI trialists. *Int J Radiat Oncol Biol Phys* 20: 1183–1190

Ashcroft T, Simpson JM, Timbrell V (1988) Simple method of estimating severity of pulmonary fibrosis on a numerical scale. *J Clin Pathol* 41: 467–470

Carney DN (1996) Chemotherapy in the management of patients with inoperable non-small cell lung cancer. *Semin Oncol* 23: 71–75

Chen Y, Okunieff P (2004) Radiation and third-generation chemotherapy. *Hematol Oncol Clin North Am* 18: 55–80

Chen Y, Pandya K, Keng PC, Johnstone D, Li J, Lee YJ, Smudzin T, Okunieff P (2003) Phase I/II clinical study of pulsed paclitaxel radiosensitization for thoracic malignancy: a therapeutic approach on the basis of preclinical research of human cancer cell lines. *Clin Cancer Res* 9: 969–975

Choy H, Akerley W, Safran H, Graziano S, Chung C, Williams T, Cole B, Kennedy T (1998a) Multiinstitutional phase II trial of paclitaxel, carboplatin, and concurrent radiation therapy for locally advanced non-small-cell lung cancer. *J Clin Oncol* 16: 3316–3322

Choy H, Devore III RF, Hande KR, Porter LL, Rosenblatt P, Yunus F, Schlabach L, Smith C, Shyr Y, Johnson DH (2000) A phase II study of paclitaxel, carboplatin, and hyperfractionated radiation therapy for locally advanced inoperable non-small-cell lung cancer (a Vanderbilt Cancer Center Affiliate Network Study). *Int J Radiat Oncol Biol Phys* 47: 931–937

Choy H, Rodriguez FF, Koester S, Hilsenbeck S, Von Hoff DD (1993) Investigation of taxol as a potential radiation sensitizer. *Cancer* 71: 3774–3778

Choy H, Safran H, Akerley W, Graziano SL, Bogart JA, Cole BF (1998b) Phase II trial of weekly paclitaxel and concurrent radiation therapy for locally advanced non-small cell lung cancer. *Clin Cancer Res* 4: 1931–1936

Cividalli A, Arcangeli G, Cruciani G, Livdi E, Cordelli E, Danesi DT (1998) Enhancement of radiation response by paclitaxel in mice according to different treatment schedules. *Int J Radiat Oncol Biol Phys* 40: 1163–1170

Dillman RO, Seagren SL, Propert KJ, Guerra J, Eaton WL, Perry MC, Carey RW, Frei III EF, Green MR (1990) A randomized trial of induction

chemotherapy plus high-dose radiation *vs* radiation alone in stage III non-small-cell lung cancer. *N Engl J Med* 323: 940–945

Dowell JE, Sinard R, Yardley DA, Aviles V, Machtay M, Weber RS, Weinstein GS, Chalian AA, Carbone DP, Rosenthal DI (1999) Seven-week continuous-infusion paclitaxel concurrent with radiation therapy for locally advanced non-small cell lung and head and neck cancers. *Semin Radiat Oncol* 9: 97–101

Early Breast Cancer Trialists' Collaborative Group (2000) Favourable and unfavourable effects on long-term survival of radiotherapy for early breast cancer: an overview of the randomised trials. Early Breast Cancer Trialists' Collaborative Group. *Lancet* 355: 1757–1770

Ellerbroek N, Martino S, Mautner B, Tao ML, Rose C, Botnick L (2003) Breast-conserving therapy with adjuvant paclitaxel and radiation therapy: feasibility of concurrent treatment. *Breast J* 9: 74–78

Formenti SC, Volm M, Skinner KA, Spicer D, Cohen D, Perez E, Bettini AC, Groshen S, Gee C, Florentine B, Press M, Danenberg P, Muggia F (2003) Preoperative twice-weekly paclitaxel with concurrent radiation therapy followed by surgery and postoperative doxorubicin-based chemotherapy in locally advanced breast cancer: a phase I/II trial. *J Clin Oncol* 21: 864–870

Furuse K, Fukuoka M, Kawahara M, Nishikawa H, Takada Y, Kudoh S, Katagami N, Ariyoshi Y (1999) Phase III study of concurrent *vs* sequential thoracic radiotherapy in combination with mitomycin, vindesine, and cisplatin in unresectable stage III non-small-cell lung cancer. *J Clin Oncol* 17: 2692–2699

Gabizon A, Chemla M, Tzemach D, Horowitz AT, Goren D (1996) Liposome longevity and stability in circulation: effects on the *in vivo* delivery to tumors and therapeutic efficacy of encapsulated anthracyclines. *J Drug Target* 3: 391–398

Hamaguchi T, Matsumura Y, Suzuki M, Shimizu K, Goda R, Nakamura I, Nakatomi I, Yokoyama M, Kataoka K, Kakizoe T (2005) NK105, a paclitaxel-incorporating micellar nanoparticle formulation, can extend *in vivo* antitumour activity and reduce the neurotoxicity of paclitaxel. *Br J Cancer* 92: 1240–1246

Hanna YM, Baglan KL, Stromberg JS, Vicini FA, A Decker D (2002) Acute and subacute toxicity associated with concurrent adjuvant radiation therapy and paclitaxel in primary breast cancer therapy. *Breast J* 8: 149–153

Kao J, Conzen SD, Jaskowiak NT, Song DH, Recant W, Singh R, Masters GA, Fleming GF, Heimann R (2005) Concomitant radiation therapy and paclitaxel for unresectable locally advanced breast cancer: results from two consecutive phase I/II trials. *Int J Radiat Oncol Biol Phys* 61: 1045–1053

Khayat D, Antoine EC, Coeffic D (2000) Taxol in the management of cancers of the breast and the ovary. *Cancer Invest* 18: 242–260

Klibanov AL, Maruyama K, Beckerleg AM, Torchilin VP, Huang L (1991) Activity of amphipathic poly(ethylene glycol) 5000 to prolong the circulation time of liposomes depends on the liposome size and is unfavorable for immunoliposome binding to target. *Biochim Biophys Acta* 1062: 142–148

Klibanov AL, Maruyama K, Torchilin VP, Huang L (1990) Amphipathic polyethyleneglycols effectively prolong the circulation time of liposomes. *FEBS Lett* 268: 235–237

Lind PA, Marks LB, Hardenbergh PH, Clough R, Fan M, Hollis D, Hernando ML, Lucas D, Piepgrass A, Prosnitz LR (2002) Technical factors associated with radiation pneumonitis after local +/− regional radiation therapy for breast cancer. *Int J Radiat Oncol Biol Phys* 52: 137–143

Lokeshwar BL, Ferrell SM, Block NL (1995) Enhancement of radiation response of prostatic carcinoma by taxol: therapeutic potential for late-stage malignancy. *Anticancer Res* 15: 93–98

Maeda H, Matsumura Y (1989) Tumoritropic and lymphotropic principles of macromolecular drugs. *Crit Rev Ther Drug Carrier Syst* 6: 193–210

Mason KA, Milas L, Peters LJ (1995) Effect of paclitaxel (taxol) alone and in combination with radiation on the gastrointestinal mucosa. *Int J Radiat Oncol Biol Phys* 32: 1381–1389

Matsumura Y, Maeda H (1986) A new concept for macromolecular therapeutics in cancer chemotherapy: mechanism of tumoritropic accumulation of proteins and the antitumor agent smancs. *Cancer Res* 46: 6387–6392

Milas L, Hunter NR, Mason KA, Kurdoglu B, Peters LJ (1994) Enhancement of tumour radioresponse of a murine mammary carcinoma by paclitaxel. *Cancer Res* 54: 3506–3510

Milas L, Hunter NR, Mason KA, Milross CG, Saito Y, Peters LJ (1995) Role of reoxygenation in induction of enhancement of tumour radioresponse by paclitaxel. *Cancer Res* 55: 3564–3568

Morton RF, Jett JR, McGinnis WL, Earle JD, Therneau TM, Krook JE, Elliott TE, Mailliard JA, Nelimark RA, Maksymiuk AW (1991) Thoracic radiation therapy alone compared with combined chemoradiotherapy for locally unresectable non-small cell lung cancer. A randomized, phase III trial. *Ann Intern Med* 115: 681–686

Penney DP, Rubin P (1977) Specific early fine structural changes in the lung irradiation. *Int J Radiat Oncol Biol Phys* 2: 1123–1132

Rodriguez M, Sevin BU, Perras J, Nguyen HN, Pham C, Steren AJ, Koechli OR, Averette HE (1995) Paclitaxel: a radiation sensitizer of human cervical cancer cells. *Gynecol Oncol* 57: 165–169

Rowinsky EK, Chaudhry V, Forastiere AA, Sartorius SE, Ettinger DS, Grochow LB, Lubejko BG, Cornblath DR, Donehower RC (1993) Phase I and pharmacologic study of paclitaxel and cisplatin with granulocyte colony-stimulating factor: neuromuscular toxicity is dose-limiting. *J Clin Oncol* 11: 2010–2020

Rowinsky EK, Donehower RC (1995) Paclitaxel (taxol). *N Engl J Med* 332: 1004–1014

Sause W, Kolesar P, Taylor SI, Johnson D, Livingston R, Komaki R, Emami B, Curran Jr W, Byhardt R, Dar AR, Turrisi III A (2000) Final results of phase III trial in regionally advanced unresectable non-small cell lung cancer: Radiation Therapy Oncology Group, Eastern Cooperative Oncology Group, and Southwest Oncology Group. *Chest* 117: 358–364

Sinclair WK, Morton RA (1966) X-ray sensitivity during the cell generation cycle of cultured Chinese hamster cells. *Radiat Res* 29: 450–474

Taghian AG, Assaad SI, Niemierko A, Kuter I, Younger J, Schoenthaler R, Roche M, Powell SN (2001) Risk of pneumonitis in breast cancer patients treated with radiation therapy and combination chemotherapy with paclitaxel. *J Natl Cancer Inst* 93: 1806–1811

Terasima T, Tolmach LJ (1963) X-ray sensitivity and DNA synthesis in synchronous populations of HeLa cells. *Science* 140: 490–492

Tishler RB, Geard CR, Hall EJ, Schiff PB (1992) Taxol sensitizes human astrocytoma cells to radiation. *Cancer Res* 52: 3495–3497

Uchino H, Matsumura Y, Negishi T, Koizumi F, Hayashi T, Honda T, Nishiyama N, Kataoka K, Naito S, Kakizoe T (2005) Cisplatin-incorporating polymeric micelles (NC-6004) can reduce nephrotoxicity and neurotoxicity of cisplatin in rats. *Br J Cancer* 93: 678–687

Weiss RB, Donehower RC, Wiernik PH, Ohnuma T, Gralla RJ, Trump DL, Baker Jr JR, Van Echo DA, Von Hoff DD, Leyland-Jones B (1990) Hypersensitivity reactions from taxol. *J Clin Oncol* 8: 1263–1268

Yu TK, Whitman GJ, Thames HD, Strom E, McNeese MD, Perkins GH, Schechter N, Kau S, Buzdar AU, Hortobagyi GN, Thomas E, Buchholz TA (2003) Clinically-relevant pneumonitis is not increased in breast cancer patients treated with sequential paclitaxel and radiation. *Int J Radiat Oncol Biol Phys* 57(2 Suppl): S127–S128

Yu TK, Whitman GJ, Thames HD, Buzdar AU, Strom EA, Perkins GH, Schechter NR, McNeese MD, Kau SW, Thomas ES, Hortobagyi GN, Buchholz TA (2004) Clinically relevant pneumonitis after sequential paclitaxel-based chemotherapy and radiotherapy in breast cancer patients. *J Natl Cancer Inst* 96: 1676–1681

Novel SN-38–Incorporating Polymeric Micelles, NK012, Eradicate Vascular Endothelial Growth Factor–Secreting Bulky Tumors

Fumiaki Koizumi,[1] Masayuki Kitagawa,[2] Takahito Negishi,[1] Takeshi Onda,[2] Shin-ichi Matsumoto,[2] Tetsuya Hamaguchi,[3] and Yasuhiro Matsumura[1]

[1]Investigative Treatment Division, Research Center for Innovative Oncology, National Cancer Center Hospital East, Kashiwa, Chiba, Japan; [2]Pharmaceutical Research Laboratories, Research and Development Group, Nippon Kayaku Co., Ltd, Kita-ku, Tokyo, Japan; and [3]Department of Medicine, National Cancer Center Hospital, Tyuo-ku, Tokyo, Japan

Abstract

7-Ethyl-10-hydroxy-camptothecin (SN-38), a biological active metabolite of irinotecan hydrochloride (CPT-11), has potent antitumor activity but has not been used clinically because it is a water-insoluble drug. For delivery by i.v. injection, we have successfully developed NK012, a SN-38-releasing nanodevice. The purpose of this study is to investigate the pharmacologic character of NK012 as an anticancer agent, especially in a vascular endothelial growth factor (VEGF)–secreting tumor model. The particle size of NK012 was ~20 nm with a narrow size distribution. NK012 exhibited a much higher cytotoxic effect against lung and colon cancer cell lines as compared with CPT-11. NK012 showed significantly potent antitumor activity against a human colorectal cancer HT-29 xenograft as compared with CPT-11. Enhanced and prolonged distribution of free SN-38 in the tumor was observed after the injection of NK012. NK012 also had significant antitumor activity against bulky SBC-3/Neo (1,533.1 ± 1,204.7 mm^3) and SBC-3/VEGF tumors (1,620.7 ± 834.0 mm^3) compared with CPT-11. Furthermore, NK012 eradicated bulky SBC-3/VEGF tumors in all mice but did not eradicate SBC-3/Neo tumors. In the drug distribution analysis, an increased accumulation of SN-38 in SBC-3/VEGF tumors was observed as compared with that in SBC-3/Neo tumors. NK012 markedly enhanced the antitumor activity of SN-38, especially in highly VEGF-secreting tumors, and could be a promising SN-38-based formulation. (Cancer Res 2006; 66(20): 10048-56)

Introduction

The antitumor plant alkaloid camptothecin (CPT) is a broad-spectrum anticancer agent that targets DNA topoisomerase I. Although CPT has shown promising antitumor activity *in vitro* and *in vivo* (1, 2), it has not been clinically used because of its low therapeutic efficacy and severe toxicity (3, 4). Among CPT analogues, irinotecan hydrochloride (CPT-11) has recently been shown to be active against colorectal, lung, and ovarian cancer (5–9). CPT-11 itself is a prodrug and is converted to 7-ethyl-10-hydroxy-CPT (SN-38), a biologically active metabolite of CPT-11, by carboxylesterases. SN-38 exhibits up to 1,000-fold more potent cytotoxic activity against various cancer cells *in vitro* than CPT-11 (10). Although CPT-11 is converted to SN-38 in the liver and tumor, the metabolic conversion rate is <10% of the original volume of CPT-11 (11, 12). In addition, the conversion of CPT-11 to SN-38 depends on the genetic interindividual variability of carboxylesterase activity (13). Thus, direct use of SN-38 might be of great advantage and attractive for cancer treatment. For the clinical use of SN-38, however, it is essential to develop a soluble form of water-insoluble SN-38. The progress of the manufacturing technology of "micellar nanoparticles" may make it possible to use SN-38 for *in vivo* experiments and further clinical use.

Passive targeting of drug delivery system is based on the pathophysiologic characteristics that are observed in many solid tumors: hypervascularity, irregular vascular architecture, potential for secretion of vascular permeability factors, and the absence of effective lymphatic drainage that prevents efficient clearance of macromolecules. These characteristics, unique to solid tumors, are believed to be the basis of the enhanced permeability and retention effect (14–17). Supramolecular structures, such as liposomes and polymeric micelles, are expected to increase the accumulation of drugs in tumor tissue through these pathophysiologic features. Polymeric micelle–based anticancer drugs have been developed in recent years (18–20), and some of them have been under evaluation for clinical trials (21–23). This carrier system can incorporate various kinds of drugs into the inner core by chemical conjugation or physical entrapment with relatively high stability, and the size can be controlled within the range of 20 to 100 nm in diameter. This range of diameters is too large to pass through normal vessel walls; therefore, the drug can be expected to reduce side effects due to a decrease in volume of distribution.

Angiogenesis is essential for the growth and metastasis of solid tumors (24). The clinical importance of angiogenesis in human tumors was shown by several reports indicating a positive relationship between the blood vessel density in the tumor mass and poor prognosis for survival in patients with various types of cancers (25–28). Furthermore, Natsume et al. (29) reported that the antitumor activities of anticancer agents, including *cis*-diammine-dichloroplatinum, vincristine, and docetaxel, were less active against vascular endothelial growth factor (VEGF)–secreting cells, SBC-3/VEGF, *in vivo* as compared with its mock transfectant (SBC-3/Neo), although the high vascularity should have been favorable for the drug delivery.

VEGF is also well known as a potent vascular permeability factor (30). The ability of supramolecular structures to accumulate in target tissue is based on the enhanced tumor angiogenesis and tumor vascular permeability that occur in solid tumors. Therefore, we hypothesized that a polymeric micelle–based drug carrier would increase its accumulation and deliver enhanced therapeutic efficacy in tumors that secrete higher levels of VEGF. In the present study, we present the superiority of NK012 over CPT-11 in a tumor model,

Requests for reprints: Yasuhiro Matsumura, Investigative Treatment Division, Research Center for Innovative Oncology, National Cancer Center Hospital East, 6-5-1 Kashiwanoha, Kashiwa, Chiba 277-8577, Japan. Phone: 81-4-7134-6857; Fax: 81-4-7134-6857; E-mail: yhmatsum@east.ncc.go.jp.

doi:10.1158/0008-5472.CAN-06-1605

especially in a VEGF-secreting tumor, and we illustrate the outstanding advantage of polymeric micelle–based drug carriers.

Materials and Methods

Drugs and Cells

SN-38 was synthesized by Nippon Kayaku Co., Ltd. (Tokyo, Japan). CPT-11 was purchased from Yakult Honsha Co., Ltd. (Tokyo, Japan). Human colon cancer cell lines WiDR, SW480, Lovo, and HT-29 and human non–small-cell lung cancer cell line A431 were purchased from American Type Culture Collection (Rockville, MD). Human small-cell lung cancer cell line SBC-3 and human non–small-cell lung cancer cell line PC-14 were kindly provided by Dr. I. Kimura (Okayama University, Okayama, Japan) and Dr. Y. Hayata (Tokyo Medical University, Tokyo, Japan), respectively. SBC-3 and PC-14 were maintained in RPMI 1640 supplemented with 10% fetal bovine serum (Cell Culture Technologies, Gaggenau-Hoerden, Germany), penicillin, streptomycin, and amphotericin B (100 units/mL, 100 μg/mL, and 25 μg/mL, respectively; Sigma, St. Louis, MO) in a humidified atmosphere of 5% CO_2 at 37°C. Other cell lines were maintained in DMEM (Nikken Bio Med. Lab., Kyoto, Japan) supplemented with 10% fetal bovine serum. SBC-3/Neo and SBC-3/VEGF were generated from SBC-3 cells that were transfected with BMG-Neo and BMG-Neo-VEGF as previously reported (29). The full-length sequence of human VEGF expressing 206 amino acids (31) was selected. SBC-3/VEGF cells express ~100 times more soluble VEGF than SBC-3/Neo and SBC-3 cells in the supernatant of cultured cells as shown by ELISA (29).

Preparation of an SN-38–Conjugated Poly(Ethylene Glycol)-Poly(Glutamic Acid) Block Copolymer for NK012 Construction

Poly(ethylene glycol)-poly(glutamic acid) block copolymer [PEG-PGlu(SN-38)] was synthesized as follows: A poly(ethylene glycol)-poly(glutamic acid) block copolymer [PEG-PGlu] was prepared according to the previously reported technique (32, 33). SN-38 was covalently introduced into the PGlu segment by the condensation reaction between the carboxylic acid on PGlu and the phenol on SN-38 with 1,3-diisopropylcarbodiimide and *N,N*-dimethylaminopyridine at 26°C. Consequently, the PGlu segment obtained sufficient hydrophobicity. Accordingly, NK012 was constructed with self-assembling PEG-PGlu(SN-38) amphiphilic block copolymers in an aqueous milieu.

Determination of the Size Distribution of NK012 and Drug Release Behavior of SN-38 from NK012

The size distribution of NK012 was measured with the dynamic light scattering method at 25°C using a Particle Sizer NICOMP 380ZLS (Particle Sizing Systems, Santa Barbara, CA). The release behavior of SN-38 from NK012 was investigated *in vitro* at 20°C or 37°C in PBS (pH 7.3) or 5% glucose solution (pH 4.6). The concentration was 0.1 mg/mL. The amount of SN-38 released from NK012 was estimated by UV measurement at 265 nm.

In vitro Growth Inhibition Assay

The growth inhibitory effects of NK012, SN-38, and CPT-11 were examined with a 3-(4,5-dimethylthiazol-2-yl)-2,5-diphenyltetrazolium bromide (MTT) assay. One hundred eighty microliters of an exponentially growing cell suspension (6×10^3/mL-12×10^3/mL) were seeded into a 96-well microtiter plate, and 20 μL of various concentrations of each drug were added. After incubation for 72 hours at 37°C, 20 μL of MTT solution (5 mg/mL in PBS) were added to each well and the plates were incubated for an additional 4 hours at 37°C. After centrifuging the plates at 200 × *g* for 5 minutes, the medium was aspirated from each well, and 180 μL of DMSO were added to each well to dissolve the formazan. The growth inhibitory effect of each drug was assessed spectrophotometrically (SpectraMax 190, Molecular Devices Corp., Sunnyvale, CA).

In vivo Growth Inhibition Assay

The animal experimental protocols were approved by the Committee for Ethics of Animal Experimentation and the experiments were conducted in accordance with the Guidelines for Animal Experiments in the National Cancer Center or Nippon Kayaku.

Experiment 1. Female BALB/c nude mice, 7 weeks old, were purchased from CLEA Japan (Tokyo, Japan). Human colorectal cancer HT-29 cells were grown as s.c. tumor in the flank of the mice. The tumors were excised from the mice and fragments were inoculated s.c. in the mouse flank. When the tumor volume reached 70 to 170 mm^3, mice were randomly divided into test groups consisting of six mice per group (day 0). Drugs were administered on days 0, 4, and 8 by i.v. injection into the tail vein. NK012 was given at doses of 30 (maximum tolerated dose), 15, and 7.5 mg/kg/d. The reference drug, CPT-11, was given at the maximum tolerated dose, 66.7 mg/kg/d, in the optimal schedule reported (34). The length (a) and width (b) of the tumor mass were measured twice a week, and the tumor volume (TV) was calculated as follows: $TV = (a \times b^2) / 2$. Relative tumor volumes at day n were calculated according to the following formula: $RTV = TV_n / TV_0$, where TV_n is the tumor volume at day n, and TV_0 is the tumor volume at day 0. Differences in relative tumor sizes between the treatment groups at day 21 were analyzed with an unpaired t test.

Experiment 2. As a hypervascular tumor model, we used SBC-3/VEGF cells. SBC-3/Neo or SBC-3/VEGF cells (10^7) were s.c. injected into the back of mice. NK012 or CPT-11 was administered when the mean tumor volumes ($n = 4$) reached a massive size of 1,500 mm^3, which gave tumors almost 1.5 cm in length. It took ~65 days for SBC-3/Neo and 20 days for SBC-3/VEGF to reach the tumor volume of 1,500 mm^3 from the day of inoculation. NK012 at a dose of 10 or 20 mg/kg/d and CPT-11 at a dose of 15 or 30 mg/kg/d were administered i.v. on days 0, 4, and 8. Differences in tumor sizes between the treatment groups and control group at day 14 were analyzed with an unpaired t test.

Histologic and Immunohistochemical Analysis

Histologic sections were taken from SBC-3/Neo and SBC-3/VEGF tumor tissues when the volumes reached 1,500 mm^3. After extirpation, tissues were fixed with 3.9% formalin in PBS (pH 7.4), and the subsequent preparations and H&E staining were done by Tokyo Histopathologic Laboratory Co., Ltd. (Tokyo, Japan). For detection of tumor blood vessels, polyclonal anti–von Willebrand factor antibody (Dako, Glostrup, Denmark) was used.

Assay for SN-38 and CPT-11 in Plasma and Tissues

Female BALB/c nude mice bearing HT-29 (as mentioned in experiment 1; $n = 3$) were used for the analysis of the biodistribution of NK012 and CPT-11. NK012 (30 mg/kg) or CPT-11 (66.7 mg/kg) was administered i.v. to the mice. Under anesthesia, blood and tumor samples were taken at 5 minutes, 1, 6, 24, 48, 72, and 168 hours after administration of NK012 and at 5 minutes, 1, 3, 6, and 24 hours after administration of CPT-11. The blood samples were collected in microtubes and immediately centrifuged at 1,600 × *g* for 15 minutes. The plasma and tumor samples were stored at −80°C until analysis.

For the biodistribution study in hypervascular tumors (experiment 2), female BALB/c nude mice ($n = 3$) bearing 1,500-mm^3 massive SBC-3/Neo and SBC-3/VEGF tumors were used. NK012 (20 mg/kg) and CPT-11 (30 mg/kg) were administered on day 0. The mice were sacrificed at 1, 6, 24, and 72 hours (day 3) after administration. The tumor, liver, spleen, upper small intestine, lung, and blood were taken and stored at −80°C until analysis.

Preparation of the free SN-38 (polymer-unbound SN-38) and CPT-11. Tumor samples were homogenized on ice using a Digital homogenizer (Iuchi, Osaka, Japan) and suspended in the mixture of 100 mmol/L glycine-HCl buffer (pH 3)/methanol (1:1, v/v) at a concentration of 5% w/w. The concentrations of free SN-38 and CPT-11 in the plasma and tumor from aliquots of the homogenates (100 μL) and plasma (50 μL) were determined by high-performance liquid chromatography. For free SN-38 (polymer-unbound SN-38) and CPT-11, proteins were precipitated with an ice-cold mixture of methanol/H_2O/$HClO_4$ (50:45:5, v/v/v) containing CPT as an internal standard. The sample was vortexed for 10 seconds, filtered through a MultiScreen Solvinert (Millipore Corp., Bedford, MA), and analyzed.

Preparation of the polymer-bound SN-38 (SN-38 remaining bound to PEG-PGlu). To permit complete release of SN-38 from the conjugate, 20 μL of plasma and 100 μL of tissue samples were diluted with 20 μL of methanol (50%, v/v) and 20 μL of NaOH (0.3 mol/L for plasma and 0.7 mol/L for tissue). The samples were incubated for 15 minutes at 25°C. After incubation, 20 μL of HCl (0.3 mol/L for plasma and 0.7 mol/L for tissue) and 60 μL of internal standard solution were added to the samples, and then the hydrolysis was filtered through a MultiScreen Solvinert. The filtrate was applied to the high-performance liquid chromatography system.

High-performance liquid chromatography. Reversed-phase high-performance liquid chromatography was done at 35°C on a Mightysil RP-18 GP column 150 × 4.6 mm (Kanto Chemical Co., Inc., Tokyo, Japan). The samples were injected into an Alliance Waters 2795 high-performance liquid chromatography system (Waters, Milford, MA) equipped with a Waters 2475 multi λ fluorescence detector. The detector was set at 365 and 430 nm (excitation and emission, respectively) for CPT-11 and CPT, and at 365 and 540 nm for SN-38. A reversed-phase column was used at 35°C. The mobile phase was a mixture of 100 mmol/L ammonium acetate (pH 4.2) and methanol [11:9 (v/v) for SN-38 in plasma and tumor, 3:2 (v/v) for CPT-11 in plasma, and 63:37 (v/v) for CPT-11 in tumor]. The flow rate was 1.0 mL/min. Peak data were recorded with a chromatography management system (Empower, Waters). Polymer-bound SN-38 was determined by subtraction of polymer-unbound SN-38 from the total SN-38 of the hydrolysate.

Pharmacokinetic and Statistical Analyses

The concentrations of SN-38 and CPT-11 in plasma and tissue were fitted to a pharmacokinetic model by the nonlinear least-square method using WinNonlin Professional software (version 4.1; Pharsight Corp., Palo Alto, CA). We used a noncompartmental analysis. The pharmacokinetic variables were calculated using the following equations (AUC_{last} was calculated by the trapezoidal rule to the last measurable data point):

$$AUC_{inf.} = \int_0^\infty C(t)dt$$

$$T_{1/2z}(\text{terminal half} - \text{life}) = 0.693/\lambda z$$

(λz is first-order rate constant associated with the terminal portion of the curve)

$$CL_{tot} = \text{Dose}/AUC_{inf.}$$

$$V_{ss} = MRT \times CL_{tot}(\text{MRT, mean residence time})$$

Data were expressed as mean ± SD. Data were analyzed with the Student's t test when the groups showed equal variances (F test) or with Welch's test when they showed unequal variances (F test). $P < 0.05$ was regarded as statistically significant. All statistical tests were two sided.

Results

Preparation and characterization of NK012. NK012 is an SN-38-loaded polymeric micelle constructed in an aqueous milieu by the self-assembly of an amphiphilic block copolymers, PEG-PGlu(SN-38). The molecular weight of PEG-PGlu(SN-38) was determined to be ~19,000 (PEG segment, 12,000; SN-38-conjugated PGlu segment, 7,000). NK012 was obtained as a freeze-dried formulation and contained ca. 20% (w/w) of SN-38 (Fig. 1*A*). The mean particle size of NK012 is 20 nm in diameter with a relatively narrow range (Fig. 1*B*). The releasing rates of SN-38 from NK012 in PBS at 37°C were 57% and 74% at 24 and 48 hours, respectively, and those in 5% glucose solution at 37°C were 1% and 3% at 24 and 48 hours, respectively (Fig. 1*C*). SN-38 is loaded by chemical bonding to the block copolymer. The bonding is phenyl ester bond, which is stable under acidic condition and labile under mild alkaline condition. These results indicate that NK012 can release SN-38 under neutral condition even without the presence of a hydrolytic enzyme and is stable in 5% glucose solution. It is suggested that NK012 is stable before administration and starts to release SN-38, the active component, under physiologic conditions after administration.

Cellular sensitivity of non–small-cell lung cancer and colon cancer cells to SN-38, NK012, and CPT-11. The IC_{50} values of NK012 for the cell lines ranged from 0.009 μmol/L (SBC-3 cells) to 0.16 μmol/L (WiDR cells). The growth inhibitory effects of NK012 are 43- to 340-fold more potent than those of CPT-11, whereas the IC_{50} values of NK012 were 2.3- to 5.8-fold higher than those of SN-38. NK012 exhibited a higher cytotoxic effect against each cell line as compared with CPT-11 (43- to 340-fold sensitivity). On the other hand, the IC_{50} values of NK012 were a little higher than those of SN-38, similar to the cytotoxic feature also reported in a previous study about micellar drugs (ref. 23; Table 1).

Antitumor activity and pharmacokinetic analysis of NK012 and CPT-11 using HT-29–bearing nude mice (experiment 1). Potent activity was observed in mice treated with NK012 at doses of 15 and 30 mg/kg (Fig. 2*A*), although neither CPT-11 at a dose of 66.7 mg/kg/d nor NK012 at a dose of 7.5 mg/kg/d exerted any significant antitumor activity *in vivo*. Comparison of the relative tumor volume at day 21 revealed significant differences between 15 mg/kg/d NK012 and 66.7 mg/kg/d CPT-11 and between 30 mg/kg/d NK012 and 66.7 mg/kg/d CPT-11 ($P < 0.05$). Although treatment-related body weight loss was observed in mice treated with each drug, body weight recovered by day 21 (Fig. 2*B*). These results clearly show the significant *in vivo* activity of NK012 against HT-29.

After injection of CPT-11, the concentrations of CPT-11 and SN-38 for plasma declined rapidly with time in a log-linear fashion. On the other hand, NK012 (polymer-bound SN-38) exhibited slower clearance (Fig. 3*A*). The clearance of NK012 in the HT-29 tumor was significantly slower and the concentration of free SN-38 was maintained at >30 ng/g even at 168 hours after injection (Fig. 3*B*). The pharmacokinetic variables of each drug in the plasma and tumor are depicted in Table 2.

Tumor-to-plasma concentration ratios (Kp) of polymer-bound and free SN-38 increased during the observation period. The highest value of Kp was achieved at 168 hours after administration, 108 for polymer-bound and 11.0 for free SN-38 (Table 3). These results indicate that NK012 can remain in the tumor tissue for a longer period and release free SN-38.

Antitumor activity and the distribution of NK012 and CPT-11 in SBC-3/Neo or SBC-3/VEGF tumors (experiment 2). To determine whether the potent antitumor effect of NK012 is enhanced in the tumors with high vascularity, we used VEGF-secreting cells SBC-3/VEGF. There was no significant difference in the *in vitro* cytotoxic activity of each drug between SBC-3/Neo and SBC-3/VEGF (Fig. 4*A*). SBC-3/VEGF tumors are reddish by gross evaluation as compared with SBC-3/Neo tumors (Fig. 4*B*). Histologic and immunohistochemical (von Willebrand factor) examination revealed that prominent leakage of erythrocytes and high vascularity were observed in SBC-3/VEGF tumor xenografts. On the other hand, SBC-3/Neo tumors have less tumor vasculatures and more interstitial space as compared with SBC-3/VEGF tumors

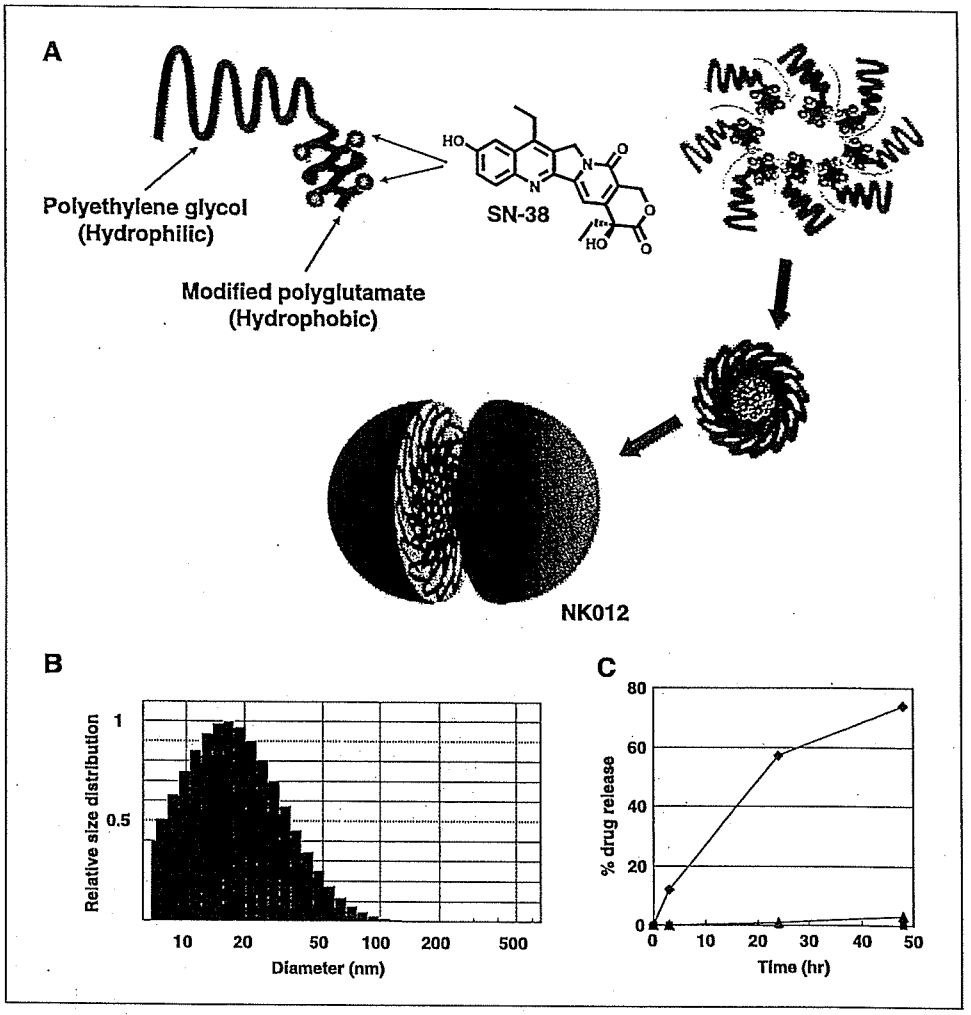

Figure 1. Preparation and characterization of NK012. *A*, schematic structure of NK012. A polymeric micelle carrier of NK012 consists of a block copolymer of PEG (molecular weight of ~12,000) and partially modified polyglutamate (~20 units). PEG (hydrophilic) is believed to be the outer shell and SN-38 was incorporated into the inner core of the micelle. *B*, size distribution of NK012 measured with the dynamic light scattering method. The *Y* axis shows relative particle size distribution. *C*, release of free SN-38 from the micelles in PBS [pH 7.3, 37°C (♦)] or 5% glucose solution [pH 4.6, 20°C (■), 37°C (▲)].

(Fig. 4*B*). Deviating from the ordinary experimental tumor model, tumors were allowed to grow until they became massive in size, ~1.5 cm (Fig. 4*C*), and then the treatment was initiated. NK012 at doses of 15 and 30 mg/kg showed potent antitumor activity against bulky SBC-3/Neo tumors (1,533.1 ± 1,204.7 mm^3) as compared with CPT-11 (Fig. 4*C*). Striking antitumor activity was observed in mice treated with NK012 (Fig. 4*C*) when we compared the antitumor activity of NK012 with that of CPT-11 using SBC-3/VEGF cells. SBC-3/VEGF bulky masses (1,620.7 ± 834.0 mm^3) disappeared in all mice, although relapse 3 months after treatment was noted in one mouse treated with NK012 20 mg/kg. On the other hand, SBC-3/VEGF were not eradicated and rapidly regrew after a partial response in mice treated with CPT-11. Approximately 10% body weight loss was observed in mice treated with 20 mg/kg NK012, but no significant difference was observed in comparison with mice treated with 30 mg/kg CPT-11.

We then examined the distribution of free SN-38 in the SBC-3/Neo and SBC-3/VEGF masses after administration of NK012 and CPT-11. In the case of CPT-11 administration, the concentrations at 1 and 6 hours after the administration were <100 ng/g both in the SBC-3/Neo and SBC-3/VEGF tumors and were almost negligible at 24 hours in both tumors (Fig. 5*A*). There was no significant difference in the concentration between the SBC-3/Neo and SBC-3/VEGF tumors. On the other hand, in the case of NK012 administration, free SN-38 was detectable in the tumors even at 72 hours after the administration. The concentrations of free SN-38 were higher in the SBC-3/VEGF tumors than those in the SBC-3/Neo tumors at any time point during the period of observation (significant at 1, 6, and 24 hours; $P < 0.05$; Fig. 5*A*).

Tissue distribution of SN-38 after administration of NK012 and CPT-11. We examined the concentration-time profile of free SN-38 in various tissues after i.v. administration of NK012 and

Table 1. *In vitro* growth inhibitory activity of SN-38, NK012, and CPT-11 in human lung and colorectal cancer cells (MTT assay)

Cell line	IC_{50} (μmol/L)		
	SN-38	NK012	CPT-11
WiDR	0.046 ± 0.008	0.16 ± 0.014	20.4 ± 1.6
SW480	0.025 ± 0.003	0.11 ± 0.028	31.9 ± 1.3
Lovo	0.0067 ± 0.0012	0.026 ± 0.003	7.24 ± 1.04
HT-29	0.016 ± 0.003	0.068 ± 0.007	23.1 ± 2.63
PC-14	0.044 ± 0.025	0.14 ± 0.021	5.96 ± 0.90
SBC-3	0.0016 ± 0.001	0.0093 ± 0.005	0.72 ± 0.22
A431	0.0081 ± 0.002	0.019 ± 0.007	5.6 ± 1.5

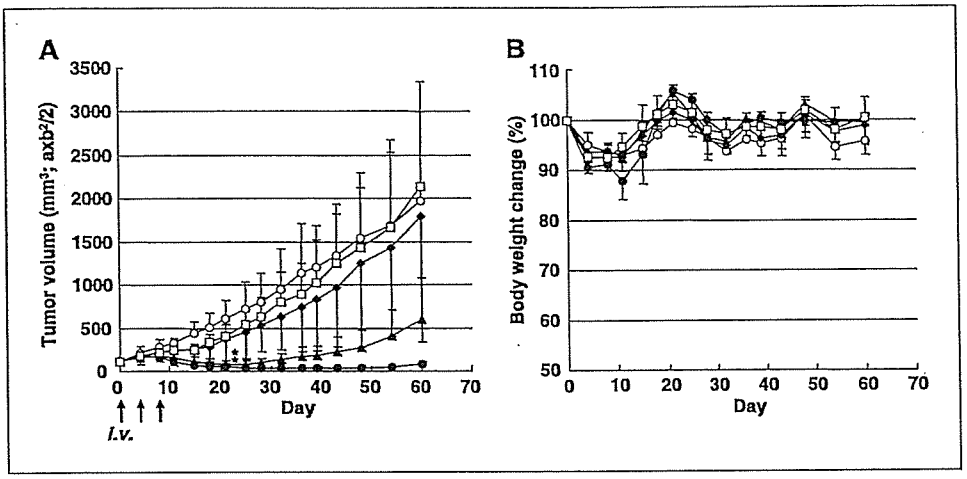

Figure 2. The effect of NK012 and CPT-11 against an HT-29 tumor xenograft. *A*, HT-29 tumor was inoculated s.c. into the flank of mice as described in Materials and Methods. CPT-11 at a dose of 66.7 mg/kg/d (□), NK012 at a dose of 7.5 mg/kg/d (♦), NK012 at a dose of 15 mg/kg/d (▲), or NK012 at a dose of 30 mg/kg/d (●) was administered i.v. on days 0, 4, and 8 (○, no treatment). Tumor volume in mice treated with CPT-11 or NK012. *Points*, mean; *bars*, SD. *, $P < 0.05$. *B*, treatment-related body weight loss occurred in mice treated with CPT-11 and NK012. *Points*, mean; *bars*, SD.

CPT-11. All organs measured exhibited the highest concentration of SN-38 at 1 hour after administration in mice given CPT-11 (Fig. 5*B*). On the other hand, mice given NK012 exhibited prolonged distribution in the liver and spleen (Fig. 5*B*). In a similar manner to other micellar drugs (19, 23), NK012 showed relatively higher accumulation in organs of the reticuloendothelial system. In the lung, kidney, and small intestine, the highest concentration of free SN-38 was achieved at 1 hour after injection of NK012 and the concentration was almost negligible at 24 hours. Although relatively high at 1 hour after administration of NK012 and CPT-11, the concentrations of free SN-38 in the small intestine rapidly decreased. Interestingly, there was no significant difference in the kinetic character of free SN-38 in the small intestine between mice treated with NK012 and CPT-11.

Discussion

The drug-incorporating polymeric micelle has characteristic pharmacokinetic features. These structures are too large to pass through normal vessel walls and evade renal excretion. The outer shell of the drug with PEG diminishes nonspecific capture by the reticuloendothelial system. Therefore, the drug can be expected to achieve a long half-life, which permits a large amount of the drug-incorporating micelles to reach the tumor site through the enhanced permeability and retention effect. The pharmacokinetic study revealed that the plasma AUC of polymer-bound SN-38 after administration of NK012 at a dose of 30 mg/kg to the HT-29-bearing mice was ~200-fold higher than that of CPT-11 at a dose of 66.7 mg/kg. A 14-fold higher AUC of the free SN-38 was achieved in mice given NK012 compared with mice given CPT-11. Prolonged circulation of NK012 in the blood might increase the accumulation of NK012 in a tumor tissue due to the enhanced permeability and retention effect. In fact, the tumor concentration of free SN-38 at 24 hours after administration of NK012 reached 90.4 ng/g and high concentrations were maintained up to 168 hours (53.1 ng/g for 48 hours, 42.6 ng/g for 72 hours, and 35.8 ng/g for 168 hours). This range of concentrations can exert sufficient antitumor activity against tumor cells. On the other hand, the concentration of CPT-11 was only 4.5 ng/g at 24 hours. These results indicate that the enhancement of tumor distribution closely contributes to the potent antitumor activity of NK012 *in vivo*.

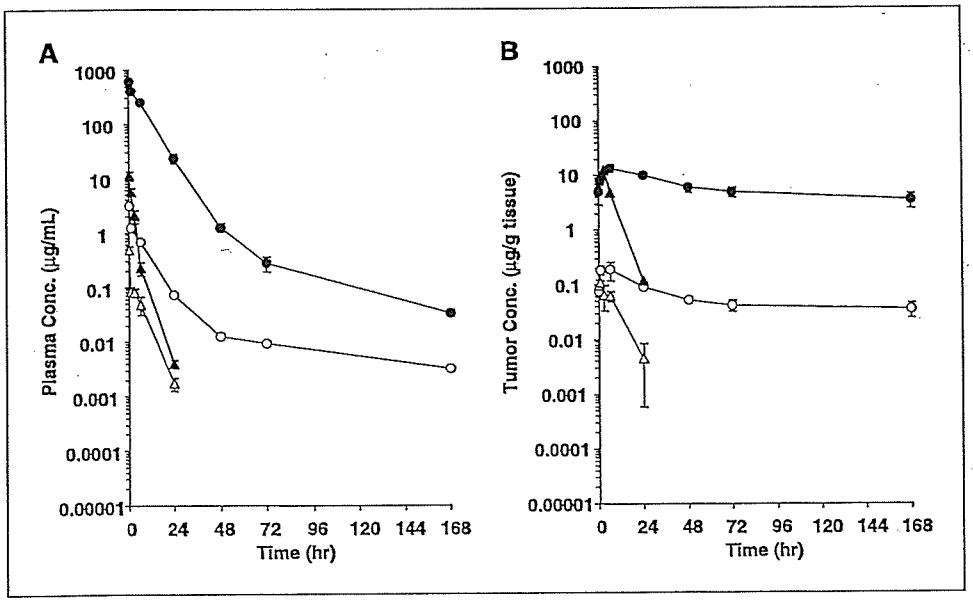

Figure 3. Plasma and tumor concentrations of respective analytes after an i.v. administration of CPT-11 (66.7 mg/kg) or NK012 (30 mg/kg) to HT-29-bearing nude mice. *A*, plasma. *B*, tumor. ●, polymer-bound SN-38; ○, free SN-38 (polymer-unbound SN-38); △, SN-38 converted from CPT-11; ▲, CPT-11.